NORGES TEKNISK-NATURVITENSKAPELIGE
UNIVERSITET

Splitting schemes for the unsteady Stokes equations: A comparison study

by

Arne Morten Kvarving

PREPRINT
NUMERICS NO. 5/2010

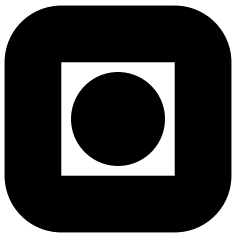

NORWEGIAN UNIVERSITY OF
SCIENCE AND TECHNOLOGY
TRONDHEIM, NORWAY

This report has URL
http://www.math.ntnu.no/preprint/numerics/2010/N5-2010.pdf
Address: Department of Mathematical Sciences, Norwegian University of Science and Technology, N-7491 Trondheim, Norway.

Splitting schemes for the unsteady Stokes equations: A comparison study

Arne Morten Kvarving

October 7, 2010

We have performed a comparison study of five velocity-pressure splitting schemes for use when solving the incompressible, unsteady Stokes equations. Different types of high order spatial discretizations have been utilized, and the schemes have been compared using two carefully crafted test problems. Particular attention has been given to the influence of different boundary conditions and discretization strategies on the accuracy and stability of the schemes. Previously, the instability of higher order schemes has been shown to be dependent on boundary conditions. We have confirmed such a coupling, however, we also have found indications that the particular spatial discretization utilized can influence their stability.

Keywords: incompressible fluid flow, velocity-pressure splitting

1 Introduction

Since the early work of Chorin [6] and Temam [22] in the 1960s, the analysis and development of velocity-pressure splitting schemes for use in simulations of incompressible fluid flows have kept many numerical analysts and scientific programmers occupied. The schemes aim to decouple the pressure and velocity leading to fast implementations, usually by using elliptic (Helmholtz and Poisson) solvers as the main ingredients. The original idea was to ignore the pressure gradient in the viscous (velocity update) step, and then update the pressure by projecting the resulting velocity field onto the space of solenoidal fields. This is known as pressure correction schemes. Over the years several improvements to the original scheme have been proposed. Goda was the first to propose adding an earlier value of the pressure gradient in the viscous update [8], naming the resulting scheme the incremental pressure correction scheme. Van Kan built on this idea and proposed a second order scheme [24], utilizing pressure extrapolants. Their ideas allow extensions to any temporal order, in principle. However, numerous problems have been reported over the years in realizing higher than second order accuracy. Timmermans et al. suggested a modification to the scheme which increases the accuracy of the pressure [23]. The main idea here is to correct the pressure for errors which surface due to the fact that we have no direct control of the divergence of the velocity on the boundary. This leads to consistent boundary conditions for the pressure including the curl of the curl of the velocity. Hence the resulting schemes are said to be on rotational form. In effect, this modification of the scheme replaces an artificial numerical boundary layer in the pressure with an inexact tangential boundary condititon for the velocity.

Other classes of schemes have been proposed over the years. Kim and Moin proposed a scheme which uses a nonhomogenous Dirichlet boundary condition in the viscous step [14]. However, as is shown in [11], this scheme is actually equivalent to the original pressure correction scheme. A big drawback with the proposed scheme is that it requires the trace of a gradient, making it ill suited for low order finite element realizations.

Karnidakis et al. [12] and Orzag et al. [18] proposed to exchange the velocity and the pressure in the original scheme, i.e., to first update the pressure ignoring the viscous terms, and then correct for viscous effects in a second step. These schemes are analogously named velocity correction schemes. As the velocity at the end of a substep is not enforced to be divergence free, this scheme cannot be classified as a projection scheme. In [12, 18] a somewhat similar scheme, named the KIO scheme, was introduced. The proposed scheme is equivalent to the velocity correction scheme on rotational form [11]. The intention was to allow extensions to higher order realizations, however just as in the rotational pressure correction scheme, the increased accuracy comes at a cost; we need access to second order derivatives, in this case in order to enforce a Neumann boundary condition on the pressure. This also means that we need approximations of the normal vector along the surface of the domain, which may not be readily available in deformed, possibly time dependent, geometries.

Guermond and Shen proposed a new class of splitting schemes in [10], and some theoretical results in the context of low order finite element discretizations can be found in [21]. These schemes are not projection schemes since the velocity at the end of a substep is not enforced to be divergence free. A nice feature of these schemes is that they lead to a trivial homogenous Dirichlet boundary condition for the velocity and a homogenous Neumann condition for the pressure update. However, on closer inspection [11] it turns out that these schemes are equivalent with work done earlier by Liu and Liu. In [25] they proposed a new formulation of the equations with the aim of eliminating the pressure from the equations. Their goal was unfortunately not completely fulfilled. The boundary conditions for the new variables imply that the these are coupled in the same fashion as the velocity and pressure are coupled in a standard formulation [11].

A final class of schemes is the schemes based on inexact algebraic factorization, originally introduced in [20, 9]. These methods have gained some popularity since they were believed to be more accurate than their PDE counter parts since they do not explicitly enforce any artificial boundary condition on the pressure. However, it turns out that they indeed enforce such a boundary condition weakly as shown in [11], and hence their equivalence with the already mentioned schemes.

The goal of this work is to compare the different splitting schemes and study how different boundary conditions and spatial discretizations might influence their behaviour, both in terms of accuracy, but also in terms of stability, in particular for higher (temporal) order realizations. There has been quite a lot of research done on these schemes earlier, as can be seen from the reference list. However, we feel that there is still some holes left when it comes to the influence of boundary conditions and spatial discretization.

We have confined our study to three classes of schemes, namely incremental pressure correction schemes, the consistent splitting schemes and the KIO scheme. These schemes were chosen since each serve to highlight different aspects of the current families of velocity-pressure decoupling schemes. The velocity resulting from an application of the pressure correction schemes on standard form is divergence free, but the pressure suffer from an improper boundary condition. If we use pressure correction on rotational form we obtain a velocity field that is incompressible and a pressure with a proper value on the boundary. However, this comes at the exponse of a velocity field which honors an incorrect tangen-

tial boundary condition. The KIO scheme yields a pressure with a proper value on the boundary, however the resulting velocity field is not divergence free. Finally, the consistent splitting schemes yield velocity fields which are not divergence free, and they do not utilize additional boundary conditions in the pressure update. A fully coupled velocity-pressure solver is used as a reference solution, even though we have an exact analytic solution we can use for convergence analysis. This to give an impression of how much we lose in terms of accuracy by utilizing the splitting schemes.

The outline of the paper is as follows. We first give a brief overview of the considered problem in Section 2. An overview of the schemes involved is given in Section 3. We then give numerical results in Section 4. Finally, in Section 5, we summarize our findings and present our conclusion.

2 The unsteady Stokes problem

We consider the incompressible, unsteady Stokes equations,

$$\frac{\mathrm{d}\mathbf{u}}{\mathrm{d}t} - \nu\nabla^2\mathbf{u} + \nabla p = \mathbf{f} \qquad \text{in } \Omega = (0, 2\pi) \times (-1, 1),$$

where, the incompressibility constraint is enforced by requiring a divergence free velocity field

$$\nabla \cdot \mathbf{u} = 0.$$

We consider the equations equipped with two different sets of boundary conditions; either periodic and no-slip conditions,

$$\begin{aligned} \mathbf{u}(x, -1) = \mathbf{u}(x, 1) &= 0, \\ \mathbf{u}(0, y) &= \mathbf{u}(2\pi, y), \\ \mathbf{u}_x(0, y) &= \mathbf{u}_x(2\pi, y), \end{aligned}$$

or pure no-slip conditions

$$\begin{aligned} \mathbf{u}(x, -1) = \mathbf{u}(x, 1) &= 0, \\ \mathbf{u}(0, y) = \mathbf{u}(2\pi, y) &= 0. \end{aligned}$$

3 Overview of the solution schemes employed

To discretize in space we employ (pseudo)spectral methods, either truncated Fourier series or expansions based on high order Legendre polynomials, in either case utilized in a Galerkin framework [7]. In time we discretize using backward differencing of order q, with $q = 1$, $q = 2$ or $q = 3$. We denote these schemes by $\frac{D}{\Delta t}$, and their coefficients are given by $\beta_i, i = 0, \cdots, q$. Thus a single ODE,

$$\frac{\mathrm{d}u}{\mathrm{d}t} = f(t, u),$$

is approximated using

$$\frac{D}{\Delta t}u^{k+1} \equiv \frac{1}{\Delta t}\sum_{i=0}^{q} \beta_i u^{k+1-i} = f(t^{k+1}, u^{k+1}).$$

As the point of reference we use a standard coupled velocity-pressure solver based on the Uzawa scheme [1, 16], where we iterate to machine precision ($\left(r^T r\right)^{\frac{1}{2}} < 10^{-16}$; here r is the residual) in the conjugate gradient (CG) solver utilized. We consider five different splitting schemes in combination with two different spatial discretizations and two different sets of boundary conditions.

3.1 The pressure correction schemes

The pressure correction schemes consist of a two step procedure, where we first extrapolate the pressure to obtain a velocity field, and then update the pressure by projecting the velocity field from the first substep onto the space of solenoidal fields [11]. On standard, incremental form the semi-discrete (discrete in time, continuous in space) equations read

$$\begin{aligned}\frac{D\hat{\mathbf{u}}^{k+1}}{\Delta t} - \nu\nabla^2\hat{\mathbf{u}}^{k+1} + \nabla p^{*,k+1} &= \mathbf{f}^{k+1},\\ \nabla^2\Delta p^{k+1} &= \frac{-\beta_0}{\Delta t}\nabla\cdot\hat{\mathbf{u}}^{k+1},\\ p^{k+1} &= p^{*,k+1} + \Delta p^{k+1},\\ \mathbf{u}^{k+1} &= \hat{\mathbf{u}}^{k+1} + \frac{\Delta t}{\beta_0}\nabla\Delta p^{k+1}.\end{aligned}$$

Here $p^{*,k+1}$ is a suitable extrapolation of the pressure at earlier time levels. A major issue with this scheme is that the resulting pressure satisfies a non-physical Neumann boundary condition [11]. This condition is due to the fact that the pressure update equation enforces

$$\nabla p^{k+1}\cdot\mathbf{n} = \nabla p^{k}\cdot\mathbf{n}$$

since it is solved as a (quasi-)Poisson equation implicitly equipped with a homogenous Neumann boundary condition. This results in a numerical boundary layer in the pressure error. It has therefore been proposed [23] to slightly modify the scheme and instead write it as

$$\begin{aligned}\frac{D\hat{\mathbf{u}}^{k+1}}{\Delta t} - \nu\nabla^2\hat{\mathbf{u}}^{k+1} + \nabla p^{*,k+1} &= \mathbf{f}^{k+1},\\ \nabla^2\phi^{k+1} &= \frac{-\beta_0}{\Delta t}\nabla\cdot\hat{\mathbf{u}}^{k+1},\\ p^{k+1} &= \phi^{k+1} + p^{*,k+1} - \nu\nabla\cdot\hat{\mathbf{u}}^{k+1},\\ \mathbf{u}^{k+1} &= \hat{\mathbf{u}}^{k+1} + \frac{\Delta t}{\beta_0}\nabla\phi^{k+1}.\end{aligned}$$

This is said to be on rotational form, because if the sum of the equations is considered, they yield

$$\frac{D\mathbf{u}^{k+1}}{\Delta t} + \nu\nabla\times\nabla\times\mathbf{u}^{k+1} + \nabla p^{k+1} = \mathbf{f}^{k+1},$$

which means the pressure conform to

$$\nabla p^{k+1}\cdot\mathbf{n} = \left(f^{k+1} - \nu\nabla\times\nabla\times\mathbf{u}^{k+1}\right)\cdot\mathbf{n}$$

on the boundary. The continuous pressure indeed satisfies this relation, hence it is consistent with the exact solution. Both schemes require a $\mathbb{P}_N/\mathbb{P}_{N-2}$ realization [17], i.e., they need a combination of spaces for the pressure and velocity satisfying the inf-sup condition [2, 3] to avoid spurious pressure modes.

3.2 The consistent splitting schemes

These were first introduced in [10], where the authors demonstrate stable first and second order implementations, but only give a rigorous proof of first order convergence. The main idea behind these schemes is to evaluate the pressure by testing the momentum equation

against the gradient of a test function. This procedure yields two different splitting schemes which are equivalent in the space continuous case, but which lead to different schemes when discretized. The first of them, hereby denoted as (2.8-2.9), reads

$$\frac{D\mathbf{u}^{k+1}}{\Delta t} - \nu\nabla^2\mathbf{u}^{k+1} + \nabla p^{*,k+1} = \mathbf{f}^{k+1},$$
$$\Big(\nabla p^{k+1}, \nabla q\Big) = \Big(\mathbf{f}^{k+1} - \nu\nabla\times\nabla\times\mathbf{u}^{k+1}, \nabla q\Big) \quad \forall\ q \in H^1(\Omega),$$

while the second, hereby denoted as (2.10-2.12), reads

$$\frac{D\mathbf{u}^{k+1}}{\Delta t} - \nu\nabla^2\mathbf{u}^{k+1} + \nabla p^{*,k+1} = \mathbf{f}^{k+1},$$
$$\Big(\nabla\Psi^{k+1}, \nabla q\Big) = \left(\frac{D\mathbf{u}^{k+1}}{\Delta t}, \nabla q\right) \quad \forall\ q \in H^1(\Omega),$$
$$p^{k+1} = \Psi^{k+1} + p^{*,k+1} - \nu\nabla\cdot\mathbf{u}^{k+1}.$$

The notation (2.8-2.9) and (2.10-2.12) refer to the equation numbers in the original paper [10], they do not refer to equations in this paper. A key difference between these two schemes is that the first scheme does not seem to be plagued by the infamous spurious pressure modes [10] and hence it can be implemented in a $\mathbb{P}_N/\mathbb{P}_N$ setting, while the second one can only be realized in a $\mathbb{P}_N/\mathbb{P}_{N-2}$ setting. Another important difference is that the second scheme explicitly corrects the pressure for errors on the boundary, just as in the rotational pressure correction scheme. The main difference between these schemes and the pressure correction schemes is that these are not projecting the velocity field onto the space of solenoidal fields, i.e., the incompressibility is only enforced in a weak sense.

3.3 The KIO schemes

These were first introduced in [12] where the authors claim unconditionally stable first and second order implementations, as well as conditionally stable third and fourth order implementations. In a follow-up article [13], the authors also offer numerical results which indicate that a third order scheme is unconditionally stable. A nice presentation of the method is given in [5]. The main idea behind these schemes is to introduce a temporary, incompressible velocity field $\hat{\mathbf{u}}^{k+1}$, evaluate the pressure by solving a Poisson equation equipped with a Neumann boundary condition before proceeding to update the velocity by solving the viscous parts of the equation for the temporary velocity field $\hat{\mathbf{u}}^{k+1}$. Note that since the temporary velocity field is incompressible, it is not explicitly included in the pressure update equation since we take the divergence. The pressure update equation reads

$$\nabla^2 p^{k+1} = \nabla\cdot\left(\mathbf{f}^{k+1} + \frac{1}{\Delta t}\sum_{i=1}^{q}\beta_i\mathbf{u}^{k+1-i}\right),$$
$$\nabla p^{k+1}\cdot\mathbf{n} = \left[\Big(\mathbf{f}^{k+1} - \nu\nabla\times\nabla\times\mathbf{u}^{*,k+1}\Big)\cdot\mathbf{n}\right],$$
$$\nabla\cdot\hat{\mathbf{u}}^{k+1} = 0,$$

where $\mathbf{u}^{*,k+1}$ denotes a suitable extrapolation of the velocity at the earlier time levels. The value for $\hat{\mathbf{u}}^{k+1}$ can be found through

$$\hat{\mathbf{u}}^{k+1} = \frac{\Delta t}{\beta_0}\left(\nabla p^{k+1} - \mathbf{f}^{k+1} - \frac{1}{\Delta t}\sum_{i=1}^{q}\beta_i\mathbf{u}^{k+1-i}\right).$$

We then proceed by solving the usual Helmholtz problem for the velocity,

$$\left(\frac{\beta_0}{\Delta t} - \nu\nabla^2\right)\mathbf{u}^{k+1} = \frac{1}{\Delta t}\hat{\mathbf{u}}^{k+1}.$$

This scheme is implemented in a $\mathbb{P}_N/\mathbb{P}_N$ setting, as the only spurious pressure mode is the hydrostatic mode. The final velocity is not projected onto the space of solenoidal fields, thus the incompressibility of the velocity field is part of the convergence process.

4 Numerical results

We here give results for the different combinations of schemes, boundary conditions and spatial discretizations. For the periodic and no-slip case we discretize using a Fourier series truncation in the periodic direction and polynomial expansion in the non-periodic direction (hereby denoted as FL). For the pure no-slip boundary conditions we use polynomial expansions in both direction (denoted as LGW).

The errors are measured using the discrete L^2-norm for the pressure, divergence and vorticity, while we employ the discrete H^1-norm for the velocity field. The norms are evaluated on a grid with twice the resolution in each spatial direction. We reconstruct the solution on the finer grid prior to evaluating the derivatives involved in the divergence and vorticity. All errors are measured relative to the reference solution on the finer grid. The exception is the divergence, which naturally is measured in an absolute fashion.

We consider two test cases, both which are inspired by the test case considered in [10]. The first case use a source function which corresponds to the exact solution

$$\begin{aligned}\mathbf{u}(x,y,t) &= \left(\sin(2\pi y)\sin^2 x \sin t, \frac{-\sin(2x)\sin^2(\pi y)\sin t}{\pi}\right),\\ p(x,y,t) &= \cos x \cos(\pi y)\sin t.\end{aligned}$$

Here the pressure has a constant normal derivative on the boundary. Some of the schemes weakly enforces this on the pressure due to solving the pressure update equation using homogenous Neumann boundary conditions. This allows us to compare these schemes to the ones which do not enforce such a condition, under favorable conditions for the former schemes. We later refer to this as the 'homogenous' test case. The other test case corresponds to the exact solution

$$\begin{aligned}\mathbf{u}(x,y,t) &= \left(\sin(2\pi y)\sin^2 x \sin t, \frac{-\sin(2x)\sin^2(\pi y)\sin t}{\pi}\right),\\ p(x,y,t) &= \sin x \sin(\pi y)\sin t.\end{aligned}$$

The pressure in this test case has a time dependent normal derivative on the boundary. This allows us to compare the schemes under favorable conditions for the second class of schemes which do not enforce a constant normal derivative. We later refer to this test case as the 'nonhomogenous' test case.

The velocity solution is in either case compatible with both periodic and no-slip boundary conditions and pure no-slip boundary conditions. All computations are started at $t = 0$ and errors are measured at time level $t_f = 1$. We use the exact solution to obtain the initial conditions and the extra initial values needed for the extrapolants. While this approach is not valid in general, we chose it here to avoid the need for extra implementation effort just to obtain initial data. This also minimizes the sources of error, i.e., we can be certain we start with the correct temporal order.

4.1 First order schemes

In their first order realization, all schemes are expected to give full first order accuracy for the pressure in the L^2-norm and the velocity in the H^1-norm [11]. We give the results for the pressure in Figure 1, the results for the vorticity in Figure 2, and the results for the velocity in Figure 3.

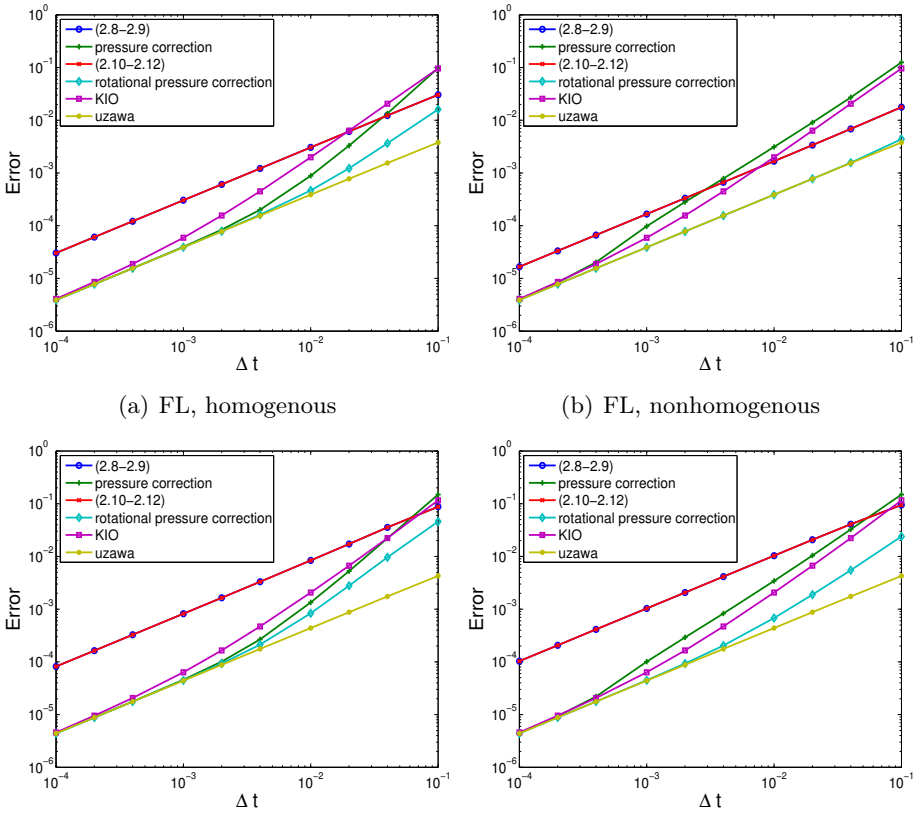

(a) FL, homogenous

(b) FL, nonhomogenous

(c) LGW, homogenous

(d) LGW, nonhomogenous

Figure 1: Errors in the pressure as a function of time step for the first order schemes. The left column show the results when we use the test problem with the homogenous pressure gradient on the boundary, while the right column show the results when we use the test problem with the nonhomogenous pressure gradient on the boundary. We have used $N = 32$ in both spatial directions to ensure the subdominance of the spatial errors.

The consistent splitting schemes are clearly the least accurate. The results for the (2.8-2.9) scheme seems to be identical with those obtained for the (2.10-2.12) scheme, independent of boundary conditions as well as the value of the exact pressure gradient on the boundary. The fact that we obtain the same results independently of the pressure gradient value is somewhat surprising, since the (2.10-2.12) scheme is not plagued by the Neumann boundary condition. The KIO scheme also seems to be fairly independent of boundary conditions and the pressure gradient value, however it is consistently more accurate than the (2.8-2.9) and (2.10-2.12) schemes. Since these schemes are the most related, in the sense that neither are projection schemes, we decided to consider the divergence given in Figure 3(e) and Figure 3(f). This seems to be the root cause of the lowered accuracy of

the consistent splitting schemes. The results are plagued by large divergence errors. The divergence seems to converge linearly in the consistent splitting schemes, while we have approximately 3/2 order convergence in the KIO scheme.

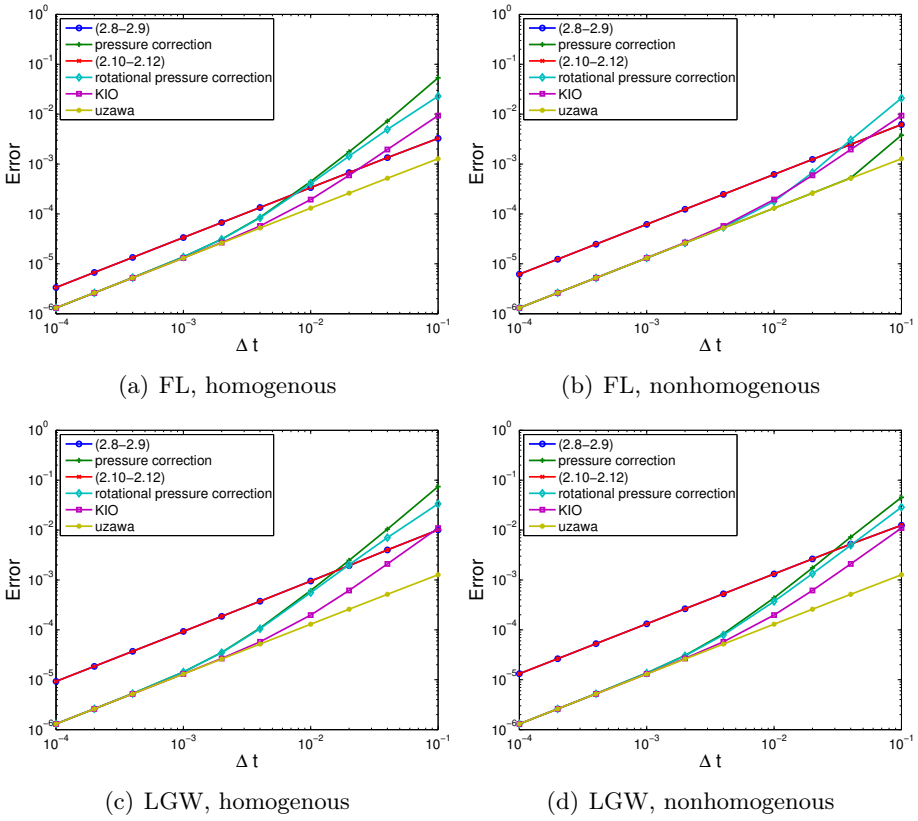

(a) FL, homogenous

(b) FL, nonhomogenous

(c) LGW, homogenous

(d) LGW, nonhomogenous

Figure 2: Error in the vorticity of the velocity field as a function of time step for the first order schemes. The left column show the results when we use the test problem with the homogenous pressure gradient on the boundary, while the right column show the results when we use the test problem with the nonhomogenous pressure gradient on the boundary. We have used $N = 32$ in both spatial directions to ensure the subdominance of the spatial errors.

The pressure correction schemes seem to be influenced by the boundary conditions as well as the value of the pressure gradient on the boundary. For the homogenous pressure gradient, they are somewhat more accurate than the KIO scheme, while this seems to have been reversed for the non-periodic case. For the non-homogenous case they are consistently more accurate than the KIO scheme. As expected, the velocity obtained for the standard form of the pressure correction scheme seems more accurate than the rotational form. Considering Figure 1, the effect of using the rotational scheme seems to be as expected, we clearly have a more accurate pressure using the rotational form for the non-homogenous pressure gradient.

The results for the vorticity seem to more or less reflect those obtained for the velocity. We note that for the periodic case with the homogenous pressure gradient, the accuracy for the consistent schemes seem to be somewhat higher than in the other cases. For the nonhomogenous pressure gradient, the pressure correction scheme seems to have a somewhat lower error with the periodic boundary conditions. It is hard to say if these are

general trends or not, in either case none of these are substantial. We conclude that the in their first order implementation, the schemes seem to perform more or less equally well, with the consistent schemes being the least accurate.

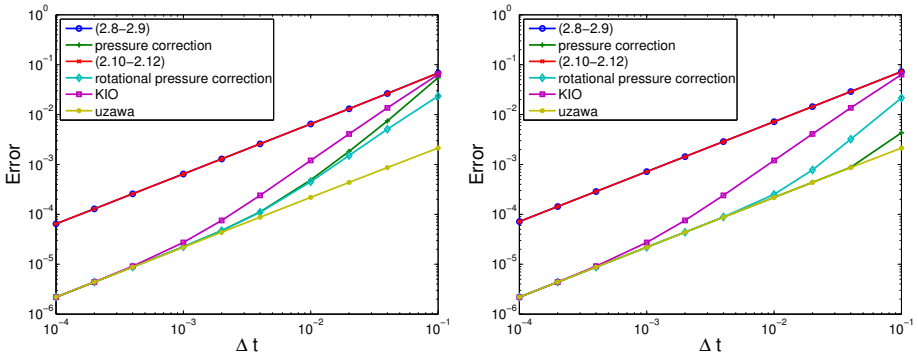

(a) FL, homogenous

(b) FL, nonhomogenous

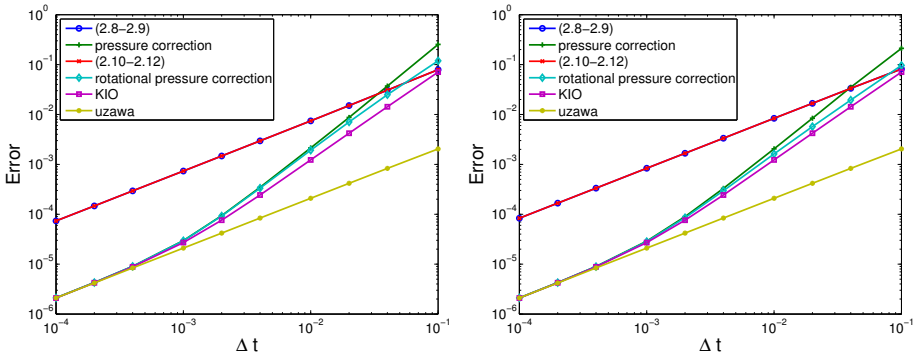

(c) LGW, homogenous

(d) LGW, nonhomogenous

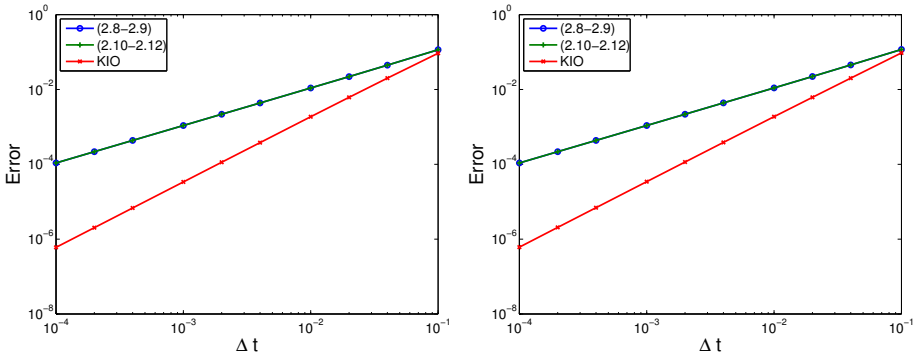

(e) FL, divergence

(f) LGW, divergence

Figure 3: Errors in the velocity as a function of time step for the first order schemes. We have used $N = 32$ in both spatial directions to ensure the subdominance of the spatial errors. Figures (a) and (c) shows the results for the homogenous test case, while figures (b) and (d) shows the results for the nonhomogenous test case. Figures (e) and (f) shows the divergence of the velocity field.

4.2 Second order schemes

We here study second order realizations of the schemes. The pressure correction schemes are expected to be fully second order accurate for the velocity in the H^1-norm, while the

pressure is formally only first order measured in the L^2-norm. Several numerical tests have indicated that the consistent schemes give full second order convergence on the velocity in the H^1-norm and the pressure in the L^2-norm, but no proof for this has been given. The KIO scheme has been proven to be of order $\Delta t^{3/2}$ for both the velocity measured in the H^1-norm, as well as the pressure measured in L^2-norm [11]. We give the results for the pressure in Figure 4, the velocity in Figure 6, and the vorticity in Figure 5.

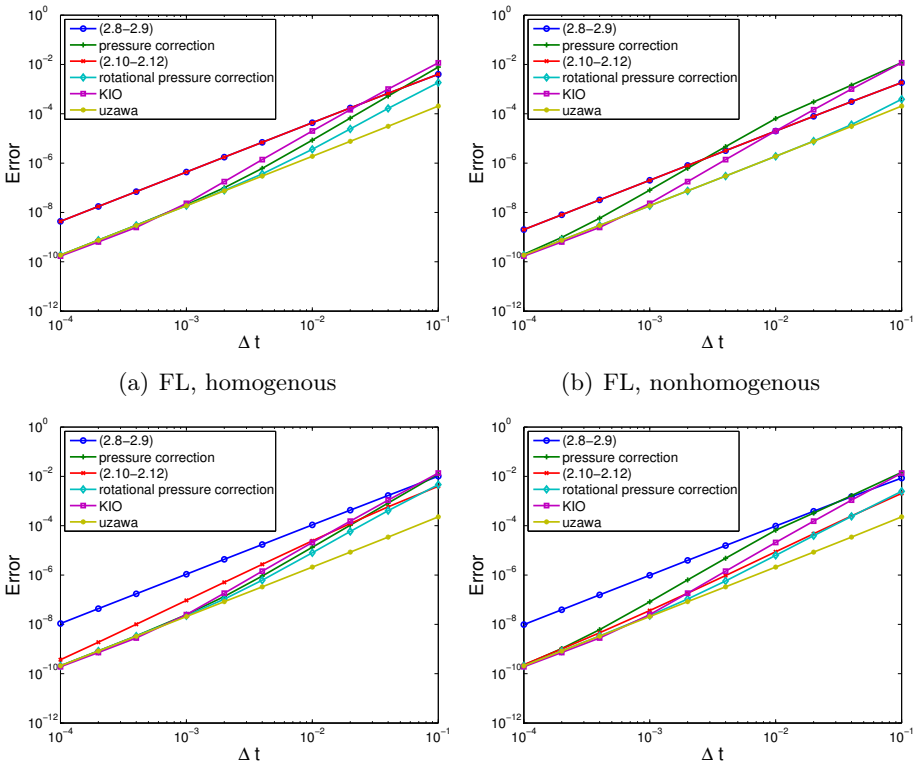

(a) FL, homogenous

(b) FL, nonhomogenous

(c) LGW, homogenous

(d) LGW, nonhomogenous

Figure 4: Errors in the pressure as a function of time step using the second order schemes. The left column show the results when we use the test problem with the homogenous pressure gradient on the boundary, while the right column show the results when we use the test problem with the nonhomogenous pressure gradient on the boundary. We have used $N = 32$ in both spatial directions to ensure the subdominance of the spatial errors.

For the consistent schemes, we now seem to have different behaviors for the different boundary conditions. They yield exactly the same results for the periodic boundary condition, while the results are different in the Dirichlet case. In [10] the authors state that the two schemes are equivalent, but only in the space continuous case. This apparent deviation from what has been reported in the literature puzzled us, so we decided to implement a periodic version of the schemes where we utilize two polynomial directions, a discretization we hereby refer to as LG. The results are given in Figure 6(e) for the homogenous case and in Figure 6(f) for the nonhomogenous case. We again obtain different results for the two methods. Thus it seems that this effect is not only a property of the boundary conditions, but also a property of the particular spatial discretization utilized. This effect can also be observed for the pressure and the vorticity. Judging by the test cases we have considered,

the consistent splitting scheme on rotational form ((2.10-2.12)) seems very competetive using polynomial expansions, while it falls in the least accurate category with the (2.8-2.9) scheme when using trigonometric expansions.

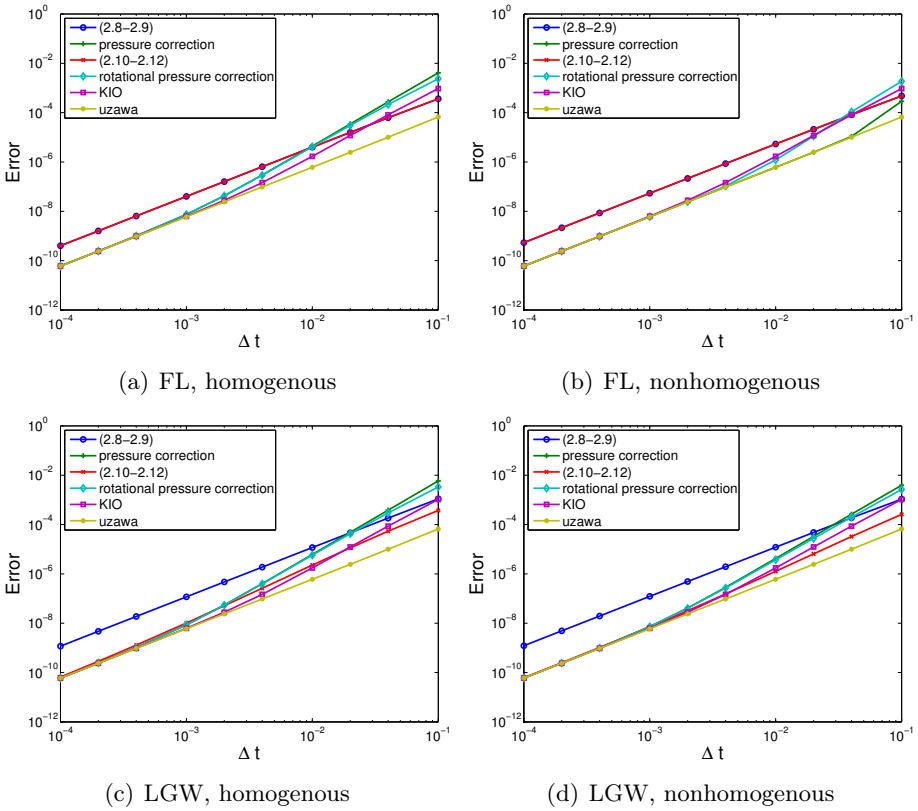

(a) FL, homogenous

(b) FL, nonhomogenous

(c) LGW, homogenous

(d) LGW, nonhomogenous

Figure 5: Error in the vorticity of the velocity field as a function of time step using the second order schemes. The left column show the results when we use the test problem with the homogenous pressure gradient on the boundary, while the right column show the results when we use the test problem with the nonhomogenous pressure gradient on the boundary. We have used $N = 32$ in both spatial directions to ensure the subdominance of the spatial errors.

The KIO scheme again seems to be fairly independent of both the value of the pressure gradient, as well as the boundary conditions. For large time steps it seems to perform consistently worse than pressure correction schemes. We can again see this reflected in large divergence errors caused by the scheme not being a projection scheme.

The pressure correction scheme seems to behave as expected, with a more accurate pressure at the expense of a less accurate velocity for the rotational scheme with the non-homogenous pressure gradient. They do not seem to exhibit any significant differences due to the boundary conditions. For the homogenous pressure gradient, they are on par with the KIO scheme, while they seem to have a slight advantage with the non-homogenous pressure gradient.

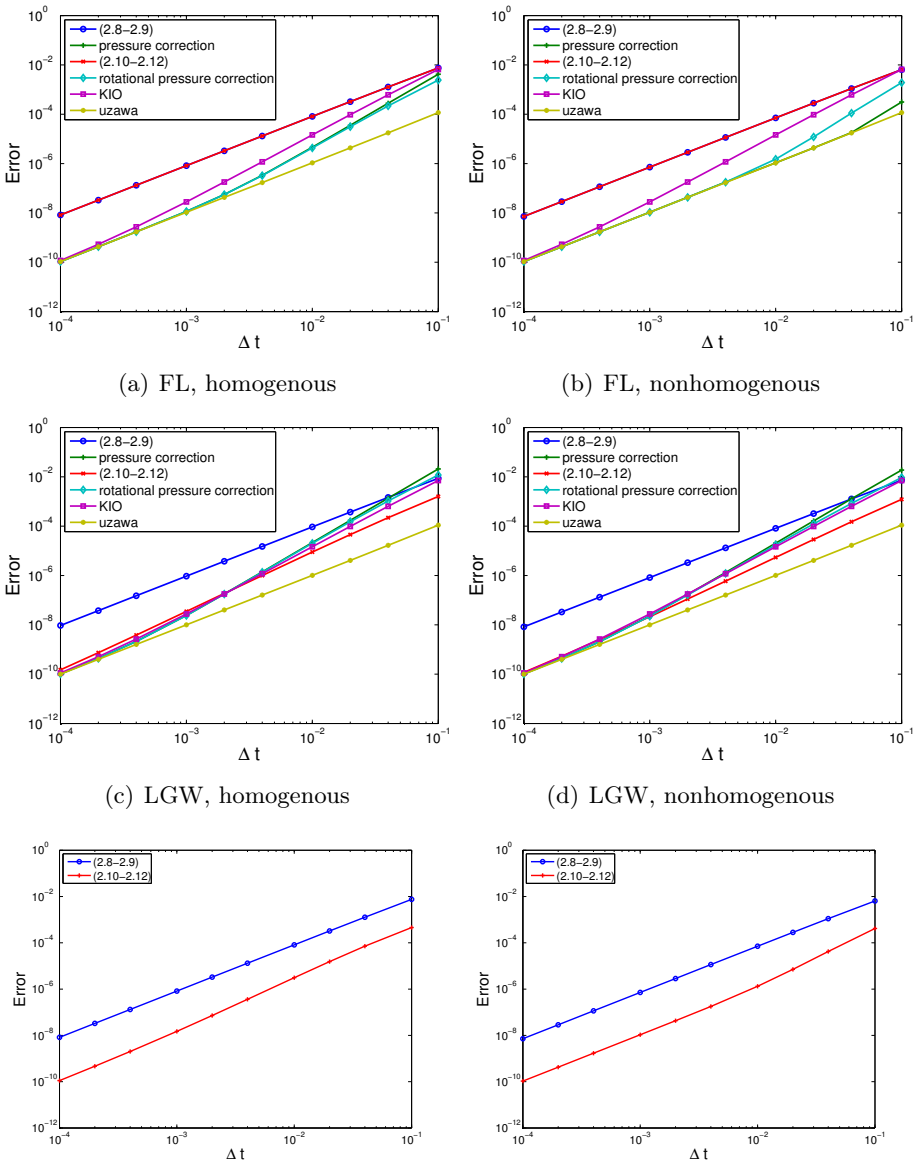

(a) FL, homogenous

(b) FL, nonhomogenous

(c) LGW, homogenous

(d) LGW, nonhomogenous

(e) LG, homogenous

(f) LG, nonhomogenous

Figure 6: Errors in the velocity as a function of time step using the second order schemes. The left column show the results when we use the test problem with the homogenous pressure gradient on the boundary, while the right column show the results when we use the test problem with the nonhomogenous pressure gradient on the boundary. We have used $N = 32$ in both spatial directions to ensure the subdominance of the spatial errors.

4.3 Third order schemes

We here give the results for the third order schemes. The (2.8-2.9) and (2.10-2.12) schemes are, as previously reported in the literature, unstable in third order realizations. We thus only have three schemes to consider; the two pressure correction schemes and the KIO scheme. The KIO scheme was developed in an attempt to obtain higher than second order schemes. In the original article [13] the authors offered numerical evidence indicating that

a third order scheme is stable, however no proof was given. On the other hand, as is pointed out in [11], due to the explicit treatment of the second order derivatives, it is reasonable to believe that this type of algorithm will only be conditionally stable. This is still an open problem. The pressure correction scheme has been shown to only be conditionally stable in a third order realization under a $\Delta t \gtrsim N^{-3}$ stability condition when supplemented with Dirichlet boundary conditions. As far as the rotational pressure correction scheme is concerned, clear consensus has not yet been established [11].

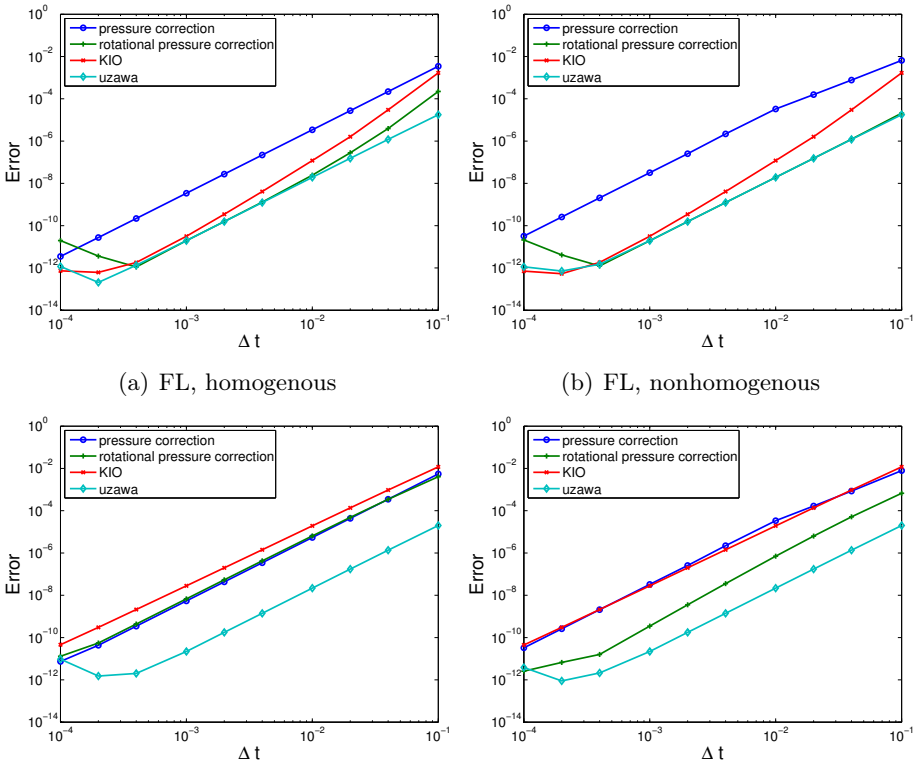

(a) FL, homogenous

(b) FL, nonhomogenous

(c) LGW, homogenous

(d) LGW, nonhomogenous

Figure 7: Errors in the pressure as a function of time step using the third order schemes. The left column show the results when we use the test problem with the homogenous pressure gradient on the boundary, while the right column show the results when we use the test problem with the nonhomogenous pressure gradient on the boundary. We have used $N = 32$ in both spatial directions to ensure the subdominance of the spatial errors.

The results for the pressure are given in Figure 7, for the velocity in Figure 8, and the vorticity in Figure 9. As predicted, we run into stability problems for the pressure correction scheme in the fully homogenous case. If we utilize a second order extrapolant, the resulting scheme is highly unstable. The results given are obtained using a linear extrapolant for the pressure. This gives a stable scheme at the cost of a much larger error constant. We have the same stability problems with the periodic boundary condition, and also here we have to reduce the extrapolant to a linear one in order to obtain a stable scheme. While the results seem to be pretty much identical for the two different boundary conditions, we have substantial differences between the two test cases. For the case with the homogenous pressure gradient, we obtain smooth convergence curves for all three fields.

For the case with the nonhomogenous pressure gradient, however, the convergence rate seems to differ for small timesteps compared to large timpe steps. The first is identified by a reduced order of convergence for the pressure, caused by the numerical boundary layer. Surprisingly, this is accompanied by a higher than third order convergence on the velocity and the vorticity. Eventually this boundary layer is overcome, and the pressure convergence order increases. This is accompanied by a jump in the error on the velocity and vorticity. Whether or not this is general behaviour is unclear to us, even after we have considered a few other test cases. The effect seemed to be there in all the cases we have considered, although less pronounced in some of them.

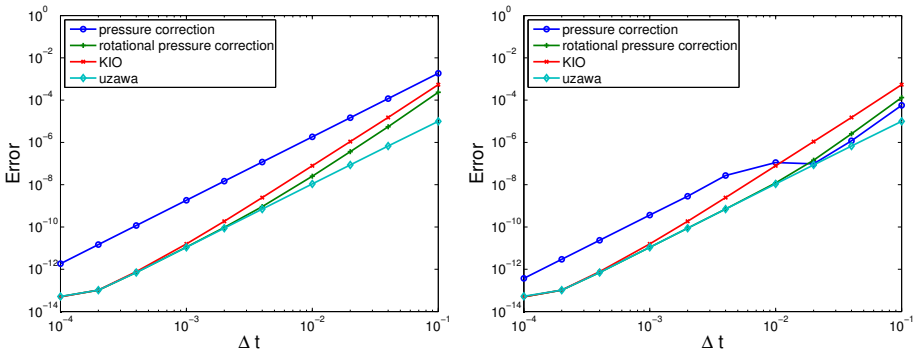

(a) FL, homogenous

(b) FL, nonhomogenous

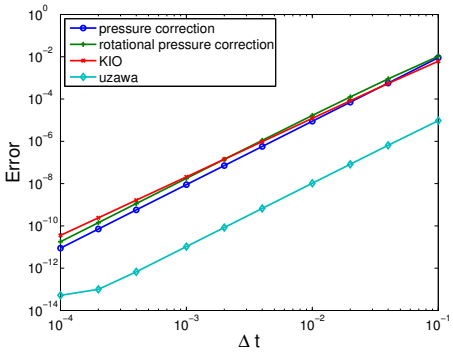

(c) LGW, homogenous

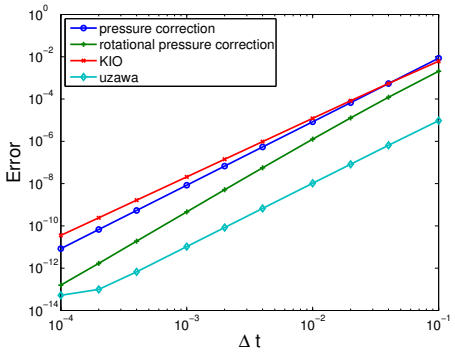

(d) LGW, nonhomogenous

Figure 8: Errors in the velocity as a function of time step using the third order schemes. The left column show the results when we use the test problem with the homogenous pressure gradient on the boundary, while the right column show the results when we use the test problem with the nonhomogenous pressure gradient on the boundary. We have used $N = 32$ in both spatial directions to ensure the subdominance of the spatial errors.

For the rotational pressure correction scheme we obtained different results for the two different boundary conditions. While a scheme utilizing a second order extrapolant seems to be unconditionally stable with the periodic boundary condition, the scheme seems to be only conditionally stable with two walls. For the latter case we again have to reduce the order of the extrapolant to obtain a stable scheme. This reduced extrapolant order significantly alters the performance of the scheme. While the scheme in general outperforms the pressure correction scheme by several orders of magnitude with the periodic boundary condition, it performs on par with the pressure correction scheme with the nonperiodic

boundary. This effect is particularly pronounced for the homogenous pressure gradient. With the nonhomogenous pressure gradient, the rotational scheme still has an advantage, in particular for the pressure due to the nonexistent boundary layer. For the velocity and vorticity, however, the scheme consistently performs worse than the non-rotational one, in particular for the larger time steps. This is another indication that using the rotational form of the scheme is not necessarily an advantage unless we are interested in a highly accurate pressure. We again wanted to see if the differences between the two realizations of the scheme are related to the particular spatial discretization utilized, rather than the boundary condition as first suspected. We thus implemented the periodic scheme using polynomial expansion in both directions. We obtained an unstable rotational pressure correction scheme, again indicating that the difference is caused by the spatial discretization used, not the boundary conditions.

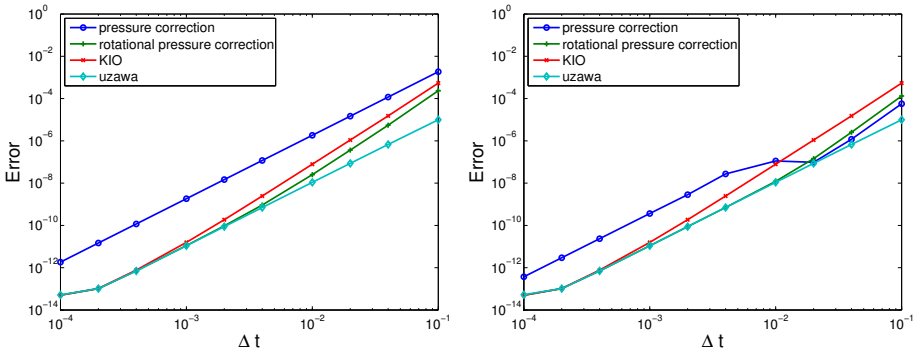

(a) FL, homogenous

(b) FL, nonhomogenous

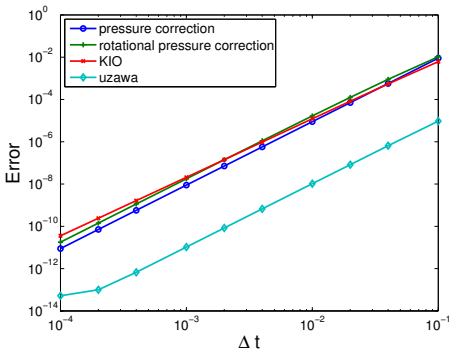

(c) LGW, homogenous

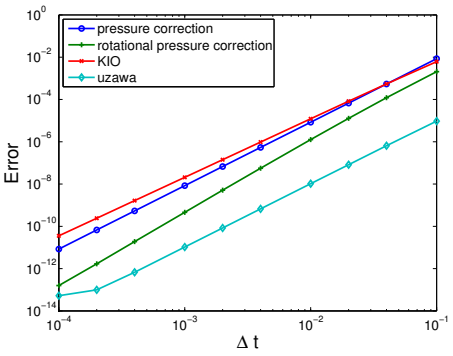

(d) LGW, nonhomogenous

Figure 9: Error in the vorticity of the velocity field as a function of time step using the third order schemes. We use the mean of a first order and a second order extrapolant for the pressure correction schemes. The exception is the rotational pressure correction scheme in its FL realization, where we use a second order extrapolant. We have used $N = 32$ in both spatial directions to ensure the subdominance of the spatial errors.

The KIO scheme behaves pretty much like the rotational pressure correction scheme as far as stability is concerned. The periodic boundary conditions allow us to use a second order extrapolant, while the nonperiodic boundary necessitates a reduction in the extrapolant order to obtain an unconditionally stable scheme. An interesting difference is that a periodic implementation using polynomial expansion in both direction here yield a stable

scheme. The KIO scheme seems to be consistently outperformed by the rotational pressure correction scheme for the test cases we have considered, with the difference being more pronounced for the cases with the nonhomogenous pressure gradient.

4.4 Comparison of the achieved orders

To get a better picture of how the different schemes behave in combination with the different spatial discretizations and boundary conditions, we here give comparative plots. In each plot a particular scheme and boundary condition/spatial realization is chosen, and results for the different orders are given. Since only three schemes (pressure correction, rotational pressure correction, KIO) are realizable in third order, we concentrate on these three schemes.

We start with the realizations of the pressure correction scheme. The results with the periodic boundary condition are given in Figure 10, while the results with the nonperiodic boundary condition are given in Figure 11. It seems we gain much accuracy by choosing a second order scheme, rather than a first order scheme. However, going from second to third order does not seem to be give us much more in terms of accuracy unless we are aiming for very low errors. There seems to be an exception for the vorticity with the nonhomogenous pressure gradient, however this advantage seems to have vanished for another test case. The results are not very surprising, since we had to reduce the order of the extrapolant to obtain stable third order schemes. In conclusion, the results indicate that second order is the highest order we can expect from a stable pressure correction scheme. If we use the rotational form of the scheme, however, this changes. The obtained orders with the periodic boundary can be seen in Figure 12, while Figure 13 shows the results obtained with the nonperiodic boundary. With the periodic boundary, it seems that using a third order scheme really gains us much in terms of accuracy. In fact, for some of the test cases, the obtained results are on par with the nonsplit approach using a relatively moderate time step of $\Delta t = \frac{1}{200}$. For the two wall case, however, the story is a bit more involved. We had to reduce the order of the extrapolant to obtain a stable scheme. This has substantially impeded the performance of the scheme, bringing it close to the performance of the second order scheme. The value of the pressure gradient on the boundary seems to influence the results. With the non-homogenous gradient, the scheme does indeed seem to behave better in a third order realization, in particular for moderate to small time steps, where the scheme has a substantial upper hand compared to the second order realization.

The picture looks pretty much the same for the KIO scheme. The results for the periodic case are given in Figure 14, while the results for the nonperiodic case are given in Figure 15. The third order scheme is consistently more accurate for the periodic boundary conditions, while the difference between the second and third order realizations are all but irrelevant with the non-periodic boundary. There seems to be no substantial influence of the value of the pressure gradient.

4.5 Efficiency of the algorithms

It is very tempting to assume that since we avoid the nested solves, the splitting schemes are always preferable to a Uzawa solver. However, with our simple geometry this is not always the case. The geometry enables us to use diagonalized solvers in the inner update which are very fast, $\mathcal{O}(N^3)$ operations for a $N \times N$ grid [15, 19]. We use a preconditioner originally introduced in [4]. This preconditioner proves extremely efficient at reducing the number of (outer) iterations and is also fast to evaluate; see Table 1. If we only consider leading order terms, each splitting scheme consists of four elliptic solves per iteration. The

Uzawa scheme consists of approximately 9 elliptic solves for the pressure (assuming we use approximately 4 iterations as the results in Table 1 indicate), four in the preconditioner, four in the residual update within the CG iteration and one in the construction of the right hand side. In addition we have the three elliptic solves for the velocity, yielding a grand total of twelve elliptic solves per iteration, as opposed to the four solves in the splitting schemes. This means that in leading order terms, to obtain a *fixed accuracy*, we cannot expect the splitting schemes to outperm the Uzawa solver if we have to increase the number of time steps with more than a factor of three.

Table 1: Mean number of iterations in the CG solver for different spatial resolutions N using the FL realization. The computations are done with $\Delta t = 10^{-3}$ and the numbers are the mean number of iterations over 1000 time steps. We obtain pretty much the same numbers for the other realizations.

N	N_{iter}, CG	N_{iter}, PCG
4	2	2
8	9.658	5
16	16.557	4
32	25.036	4
48	32.378	4
64	38.656	4

It turns out that we can run into situations where the Uzawa solver outperforms some of the splitting schemes, in particular the consistent splitting schemes, for some fixed error target. We use the case with the homogenous pressure gradient as an example. Figure 16 shows a plot in the error-solves plane. It is evident that for some error targets splitting actually hurts the performance rather than improving it. In particular this is evident for the first order scheme, where any error target lower than approximately $\|e\| < 10^{-3}$ seems to be achieved using less elliptic solves with a nonsplit approach than with. After this threshold, splitting seems to reach the specified error target at a lower cost. The exception is the consistent schemes which seems to be more expensive than a nonsplit approach for all error targets considered. For the second order schemes, this threshold is far less pronounced, splitting seems to be beneficial for any error target below approximately $\|e\| < 10^{-5}$. There seems to be only minor differences between the two boundary conditions, the main exception is the better performance of the (2.10-2.12) scheme with the nonperiodic boundary.

For the third order schemes there are substantial differences between the two boundary conditions, due to the reduced order of the extrapolant used for the non-periodic boundary. While splitting using the rotational pressure correction or the KIO scheme seems to be beneficial for all error targets with the periodic boundary condition, splitting seems to be consistently more expensive for the two wall case.

Whether or not these observations are valid for problems in more general geometries is not easy to answer in general. Since larger, more general problems usually make iterative solution of the linear systems a necessity, the cost of inverting the different elliptic operators cannot be as easily compared. In particular, we generally have better preconditioners for inverting the Laplacian than we do for inverting the consistent pressure operator, which could make the pressure correction schemes relatively more costly. On the other hand, there is no guarantee that the Cahouet preconditioner [4] would perform as good for the Uzawa operator. The KIO scheme requires access to second order derivatives as well as the

normal derivatives on the border of the domain. Obtaining these might be a challenging task in general geometries, and may potentially be quite expensive. The consistent splitting schemes only utilize standard Laplacian operators and do not require access to neither higher order derivatives nor normal derivatives, which may make these schemes more competetive. These are important aspects to keep in mind. Depending on your application splitting might not always be beneficial for the overall performance of your program.

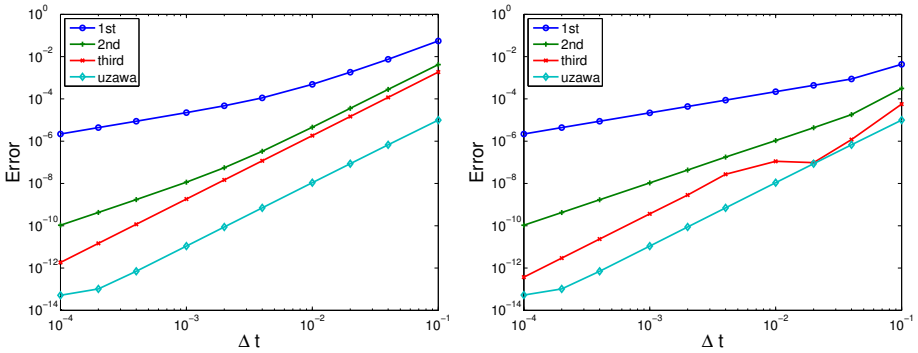

(a) pressure, homogenous

(b) pressure, nonhomogenous

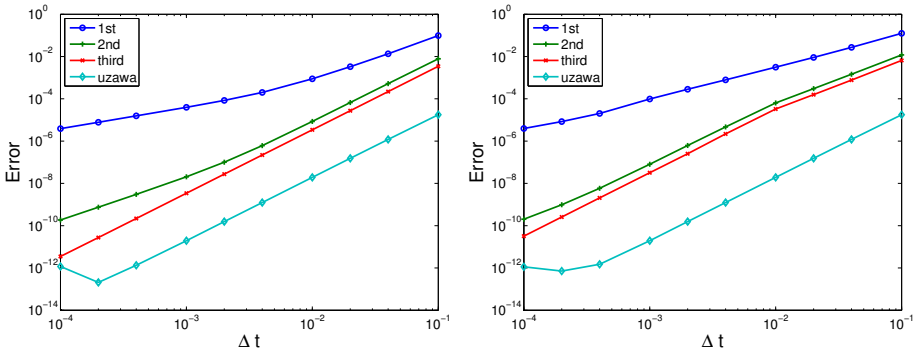

(c) velocity, homogenous

(d) velocity, nonhomogenous

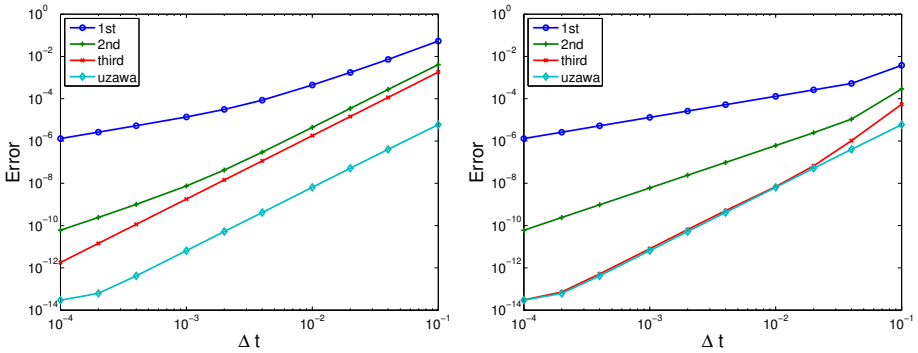

(e) vorticity, homogenous

(f) vorticity, nonhomogenous

Figure 10: Errors as a function of time step using the FL implementations of the pressure correction schemes. The third order Uzawa solution is given as a reference.

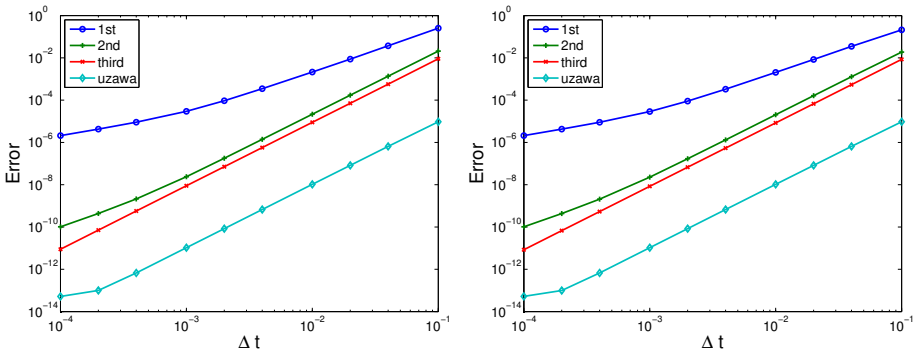

(a) pressure, homogenous

(b) pressure, nonhomogenous

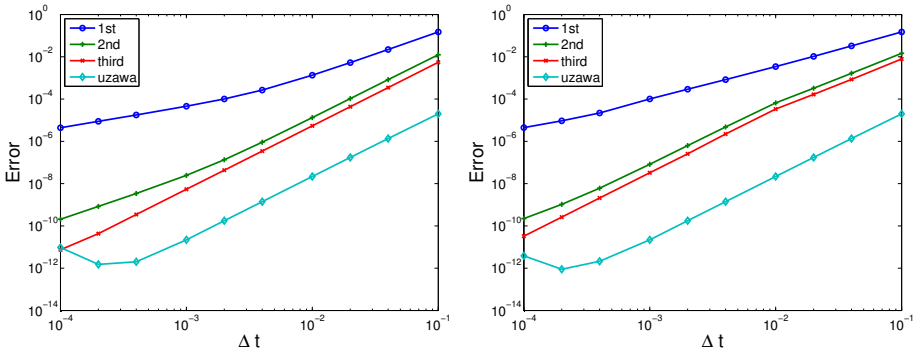

(c) velocity, homogenous

(d) velocity, nonhomogenous

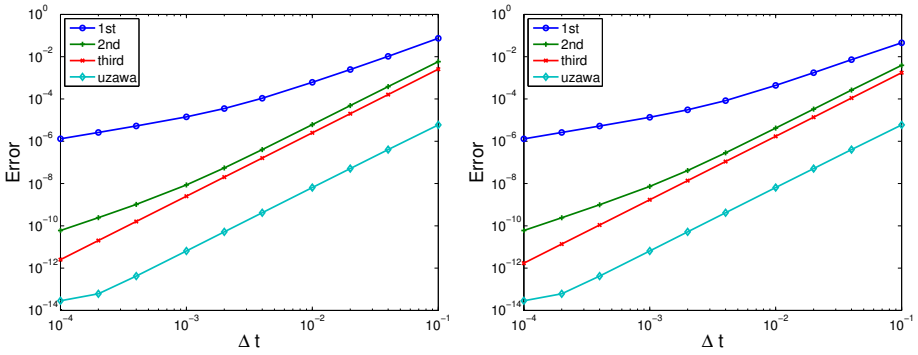

(e) vorticity, homogenous

(f) vorticity, nonhomogenous

Figure 11: Errors as a function of time step using the LGW implementations of the pressure correction schemes. The third order Uzawa solution is given as a reference.

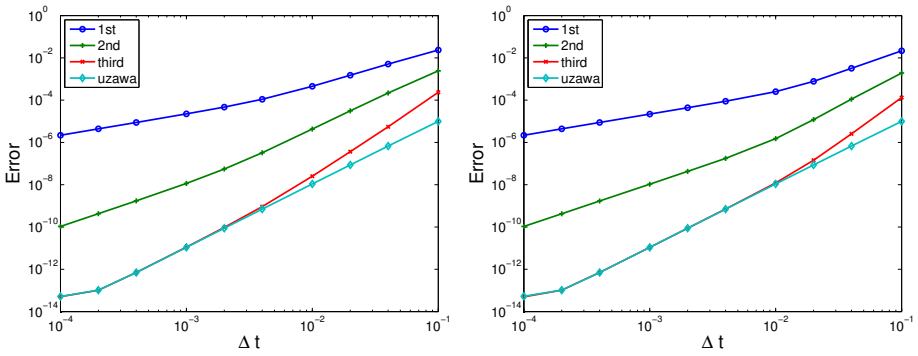

(a) pressure, homogenous

(b) pressure, nonhomogenous

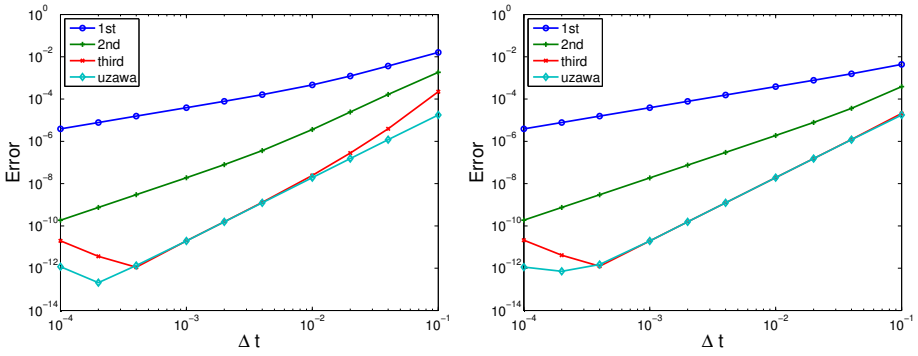

(c) velocity, homogenous

(d) velocity, nonhomogenous

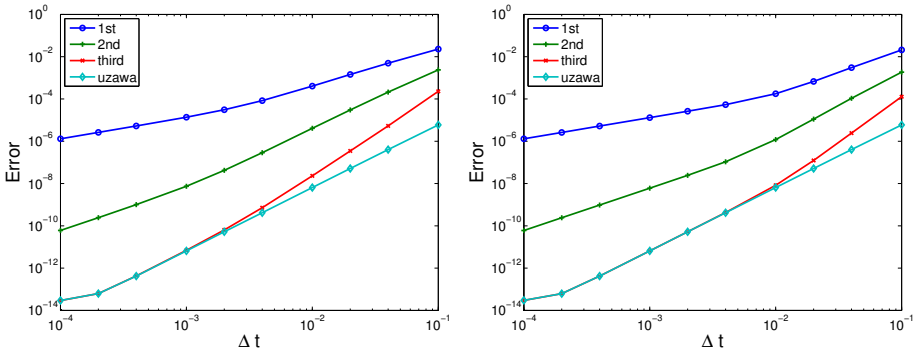

(e) vorticity, homogenous

(f) vorticity, nonhomogenous

Figure 12: Errors as a function of time step using the FL implementations of the rotational pressure correction schemes. The third order Uzawa solution is given as a reference.

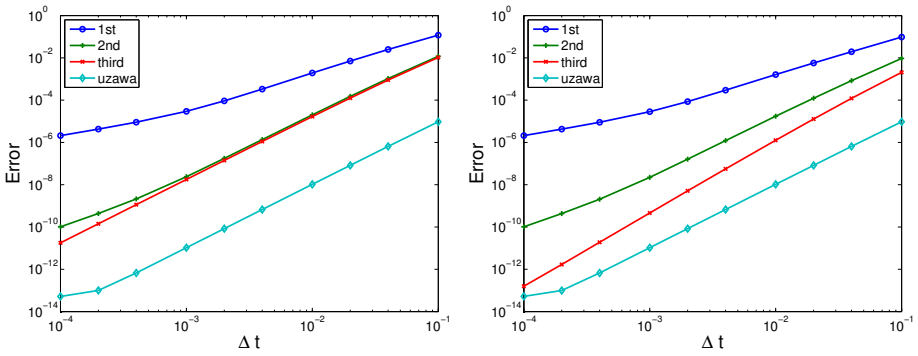

(a) pressure, homogenous

(b) pressure, nonhomogenous

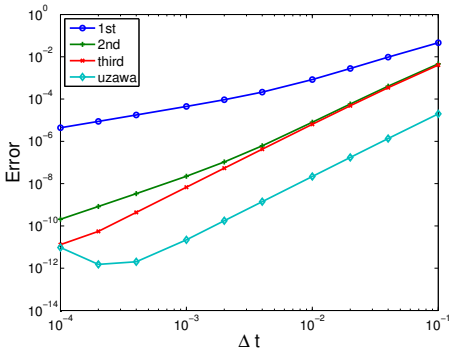

(c) velocity, homogenous

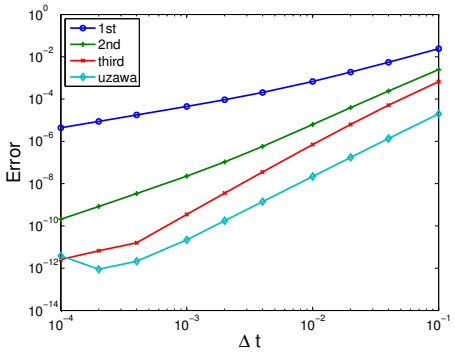

(d) velocity, nonhomogenous

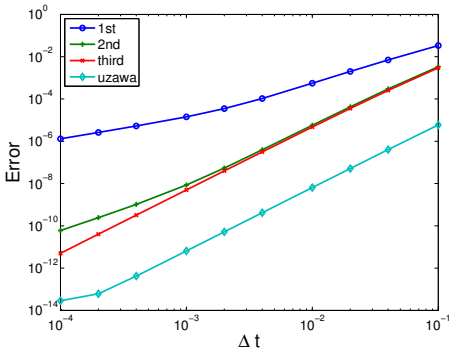

(e) vorticity, homogenous

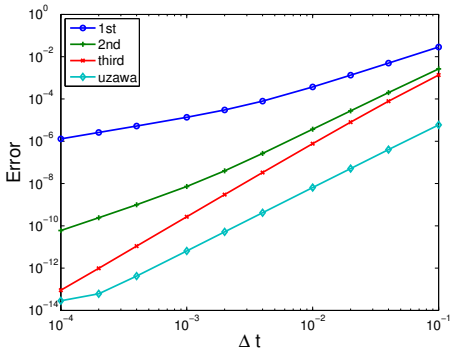

(f) vorticity, nonhomogenous

Figure 13: Errors as a function of time step using the LGW implementations of the rotational pressure correction schemes. The third order Uzawa solution is given as a reference.

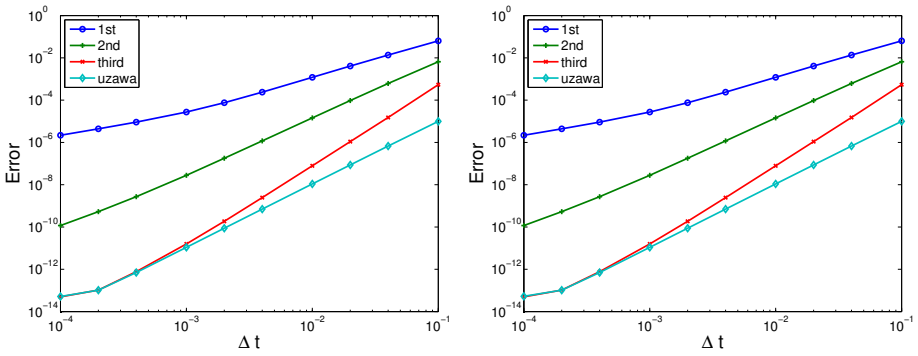

(a) pressure, homogenous

(b) pressure, nonhomogenous

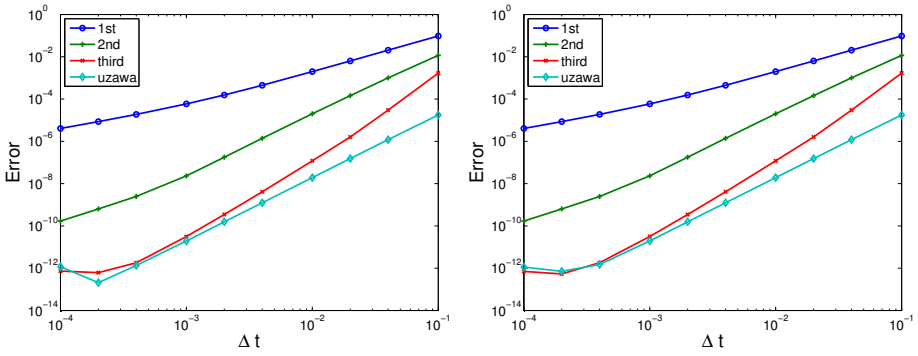

(c) velocity, homogenous

(d) velocity, nonhomogenous

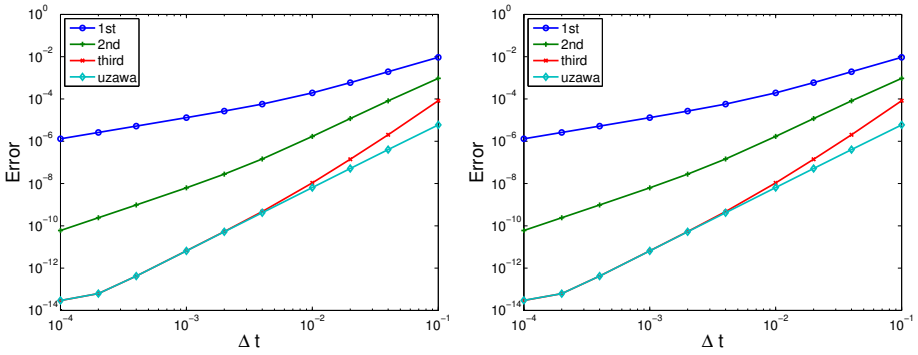

(e) vorticity, homogenous

(f) vorticity, nonhomogenous

Figure 14: Errors as a function of time step using the FL implementations of the KIO schemes. The third order Uzawa solution is given as a reference. We have used $N = 32$ in both spatial directions to ensure the subdominance of the spatial errors.

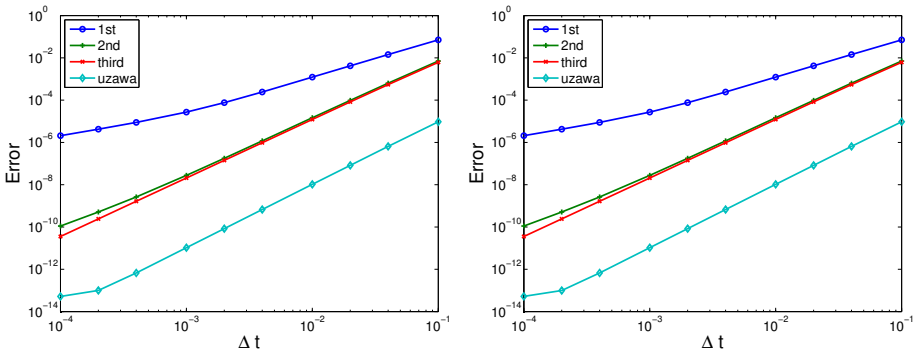

(a) pressure, homogenous

(b) pressure, nonhomogenous

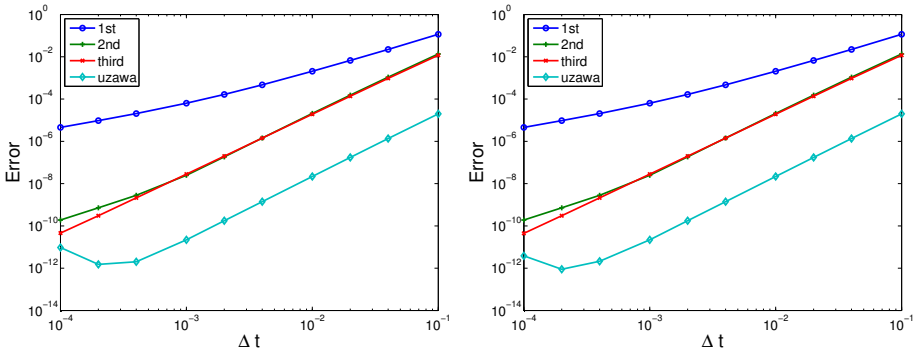

(c) velocity, homogenous

(d) velocity, nonhomogenous

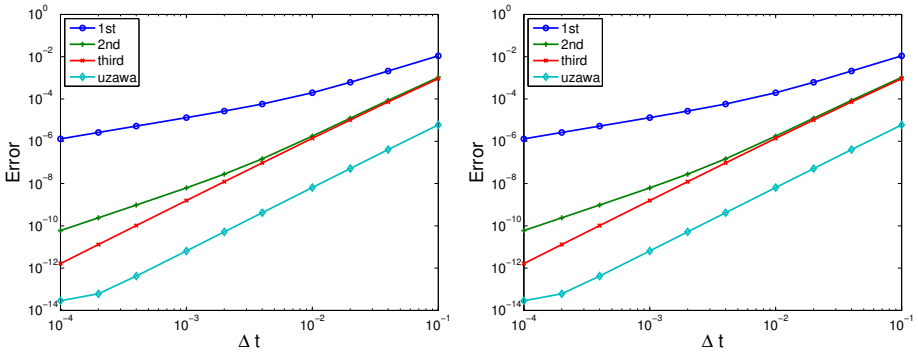

(e) vorticity, homogenous

(f) vorticity, nonhomogenous

Figure 15: Errors as a function of time step using the LGW implementations of the KIO schemes. The third order Uzawa solution is given as a reference. We have used $N = 32$ in both spatial directions to ensure the subdominance of the spatial errors.

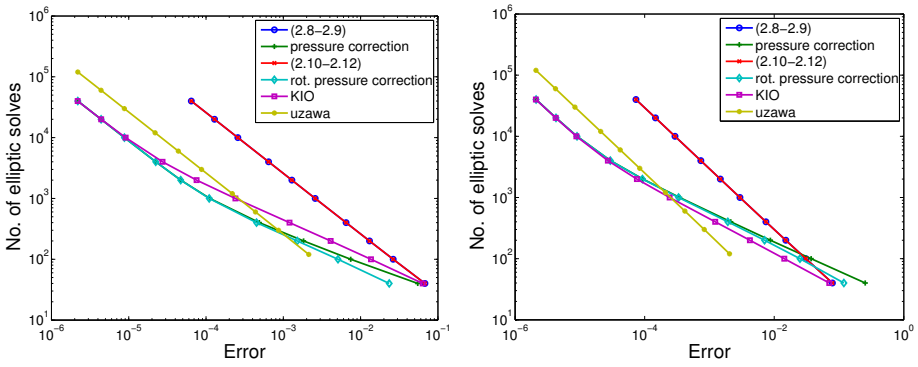

(a) first order, FL (b) first order, LGW

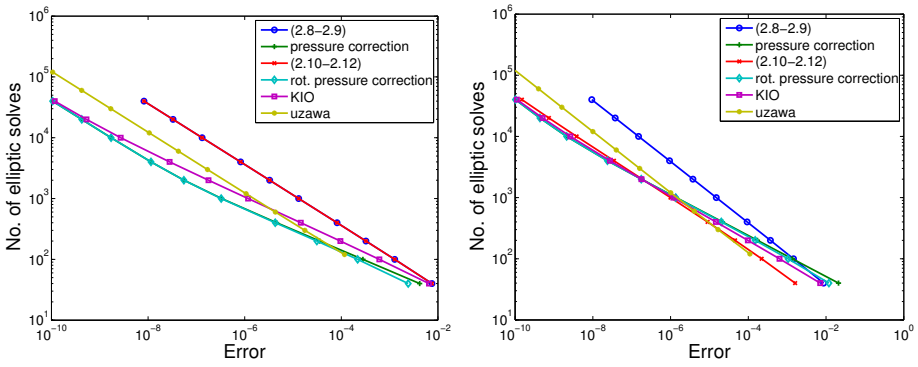

(c) second order, FL (d) second order, LGW

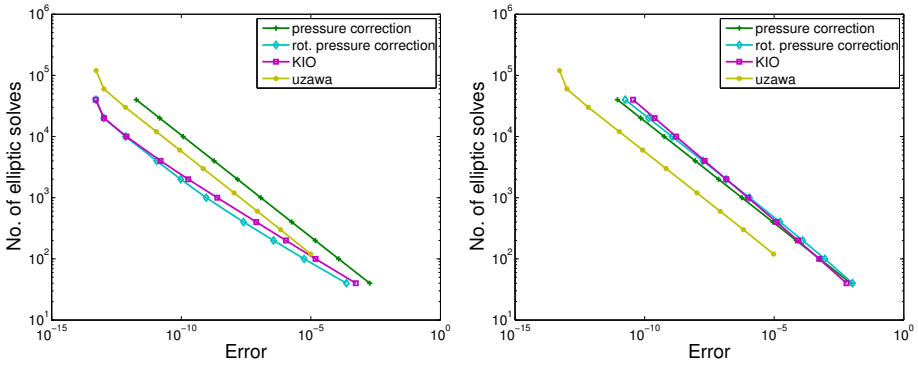

(e) third order, FL (f) third order, LGW

Figure 16: Number of elliptic solves needed to obtain specific accuracy using the different schemes in their first, second and third order realizations. The left column shows the results for the periodic boundary condition, while the right column shows the results for the non-periodic boundary condition. We have here assumed that the Uzawa solves performs exactly 4 iterations in the pressure update per time level.

5 Summary and conclusions

In this paper we have tested and compared 5 different splitting schemes for the incompressible, unsteady Stokes equations. In their first and second order realizations, we have not found any major differences in their behavior compared to what has been reported earlier in the literature. The exception was the (2.10-2.12) scheme, where we found indications that its behaviour depends on the spatial discretization utilized, a fact that seems to have gone unnoticed earlier.

Several of the schemes have been reported to have stability problems when higher than second order realizations are utilized. Our tests have confirmed the presence of such instabilities. However, we have again obtained indications that the observed instabilities also have a close coupling to the particular spatial discretization utilized, rather than being a consequence of the boundary conditions alone, as previously speculated in the literature.

Judging by our test problems, we question the general recommendation that rotational versions of the schemes should always be used. On several test problems we have seen that, while the pressure approximation does indeed improve using a rotational scheme, this comes at a cost of accuracy in the velocity due to the incorrect tangential boundary condition. In many applications, the pressure is only considered as a "necessary evil" and it is not of direct interest. The velocity, however, is seldom irrelevant, and thus we often prefer a more accurate velocity approximation. If this is the case, our tests indicate that a non-rotational scheme could be a better choice.

Finally we have seen that applying a splitting scheme may not always be beneficial for the overall efficiency of your program. The increase in the number of time steps required to reach a fixed error target may outweigh the increased cost of the solution at each time level if a non-split approach is chosen.

6 Acknowledgement

The author would like to thank Professor Einar M. Rønquist for many helpful comments and suggestions. The work has been supported by the Norwegian University of Science and Technology and the Research Council of Norway under contract 159553/I30. The support is gratefully acknowledged.

References

[1] K. Arrow, L. Hurwicz, and H. Uzawa. *Studies in Nonlinear programming.* Standford University Press, 1958.

[2] I. Babuska. The finite element method with Lagrangian multipliers. *Numer Math.*, 20, 1972/1973.

[3] F. Brezzi. On the existence, uniqueness and approximation of saddle-point problems arising from Lagrangian multipliers. *Rev. Francaise Automat. Informat. Recherche Operationelle Ser Rouge*, 8, 1974.

[4] J. Cahouet and J. P. Chabard. Some fast 3d finite element solvers for the generalized Stokes problem. *Intl. J. Numer. Met. Fluids*, 8, 1988.

[5] C. Canuto, M. Y. Hussaini, A. Quarteroni, and T. A. Zang. *Spectral Methods: Evolution to Complex Geometries and Applications to Fluid Dynamics.* Springer-Verlag, 2007.

[6] A. J. Chorin. Numerical solution of the Navier-Stokes equations. *Math. Comput*, 22, 1968.

[7] B. Galerkin. Rods and plates: Series occurring in various questions concerning the elastic equilibrium of rods and plates. *Vestn. Inzhen*, 1915.

[8] K. Goda. A multistep technique with implicit difference schemes for calculating two- or three-dimensional cavity flows. *J. Comput. Phys.*, 30, 1979.

[9] P. M. Gresho and S. T. Chan. On the theory of semi-implicit projection methods for viscous incompressible flow and its implementation via finite element method that also introduces a nearly consistent mass matrix. part i and part ii. *Intl. J. Numer. Meth. Fluids*, 11, 1990.

[10] J. L. Guermond and J. Shen. A new class of truly consistent splitting schemes for incompressible flows. *J. Comput. Phys.*, 2003.

[11] J. L. Guermond, J. Shen, and P. Minev. An overview of projection methods for incompressible flows. *Comp. Met. Mech. Eng.*, 2005.

[12] G. E. Karniadakis, M. Israeli, and S. A. Orszag. High-order splitting methods for the incompressible Navier-Stokes equations. *J. Comput. Phys.*, 1991.

[13] G. E. Karniadakis, M. Israeli, and S. A. Orszag. High-Order Splitting Methods for the Incompressible Navier-Stokes Equations. *J. Comput. Phys.*, 97:414–443, 1991.

[14] J. Kim and P. Moin. Application of a fractional-step method to incompressible Navier-Stokes equations. *J. Comput. Phys.*, 59, 1985.

[15] R. E. Lynch, J. R. Rice, and D. H. Thomas. Direct solution of partial difference equations by tensor product methods. *Numer. Math.*, 6:185–199, 1964.

[16] Y. Maday, D. Meiron, A. T. Patera, and E. M. Rønquist. Analysis of iterative methods for the steady and unsteady Stokes problem: Application to spectral element discretizations. *J. Sci. Comput.*, 14:310–337, 1993.

[17] Y. Maday, A. T. Patera, and E. M. Rønquist. The $P_N \times P_{N-2}$ method for the approximation of the Stokes problem. Technical Report 92009, Department of Mechanical Engineering, Massachusetts Institute of Technology, 1992.

[18] S. A. Orszag, M. Deville, and M. Israeli. Boundary conditions for incompressible flows. *J. Sci. Comput.*, 1, 1986.

[19] S.A. Orszag. Spectral methods for problems in complex geometries. *J. Comput. Phys.*, 37:70–92, 1980.

[20] J. B. Perot. An analysis of the fractional step method. *J. Comput. Phys.*, 108, 1993.

[21] J. Shen and X. Yang. Error estimates for finite element approximations of consistent splitting schemes for incompressible flows. *Discrete and continuous dynamical systems - Series B*, 8, 2007.

[22] R. Temam. Sur l'approximation de la solution des équations de Navier-Stokes par la méthode des par fractionnaires ii. *Arch. Ration. Metch. Anal*, 33:377–385, 1969.

[23] L. J. P. Timmermans, P. D. Minev, and F. N. Van De Vosse. An approximate projection scheme for incompressible flow using spectral elements. *Intl. J. Numer. Met. Fluids*, 22, 1996.

[24] J. van Kan. A second-order accurate pressure-correction scheme for viscous incompressible flow. *J. Sci. Stat. Comput.*, 3, 1986.

[25] E. Weinan and J. G. Liu. Gauge method for viscous incompressible flows. *Commun. Math. Sci.*, 1, 2003.